Brain Tumor clean-APT and NOE-CEST Imaging at 7T

Craig K Jones[1,2], Domenico Zacà[3], Jun Hua[1,2], Jinyuan Zhou[1,2], Peter van Zijl[1,2], and Jay J Pillai[4]

[1]Department of Radiology and Radiological Sciences, Johns Hopkins University School of Medicine, Baltimore, MD, United States, [2]FM Kirby Center, Kennedy Krieger Institute, Baltimore, MD, United States, [3]Center for Mind Brain Sciences, University of Trento, Trento, Italy, Italy, [4]Division of Neuroradiology, Johns Hopkins University School of Medicine, Baltimore, MD, United States

Introduction: Amide proton transfer (APT) CEST has been used to successfully detect tumors[1-3] and the effect of radiation necrosis[4]. However, the mechanism of contrast is still somewhat inconclusive. When using low power RF pulses that slowly saturate protons with minimal interference of conventional semi-solid based magnetization transfer contrast (MTC),[5,6] saturation-transfer signals are revealed upfield from water in addition to the usual downfield CEST/APT signals. The visibility of such upfield signals indicates the presence of a transfer mechanism to the water signal, while their finite width indicates that these signals are likely due to mobile solutes. These effects have been attributed to saturation relayed by intramolecular nuclear Overhauser enhancements (NOE) in mobile macromolecules to water[7] either directly via dipolar transfer or relayed via exchangeable protons. Here we mapped the amide proton (clean-APT) and NOE transfer effects using low power pulsed saturation with very small MT contributions and by fitting the Z-spectrum without asymmetry analysis in an alternative effort to study protein-based signals in an infiltrating tumor.

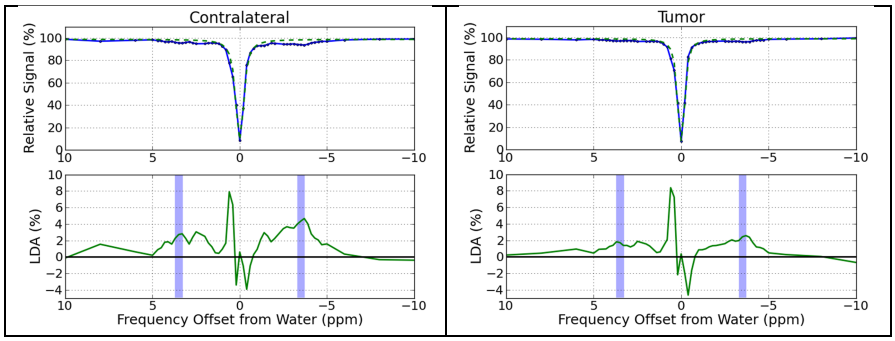

Fig. 1: Z-spectrum and Lorentzian fit (upper plots, blue and green respectively) and Lorentzian difference for a region contralateral to the tumor (left) and a region in the tumor (right). There is a decrease in both the downfield and upfield LDA in the region of the exchangeable protons (3.5 ppm) and upfield in the NOE region.

Methods: A 30 year old male with a left occipital lobe infiltrating astrocytoma with early anaplastic transformation (histopathology confirmed WHO Grade III) was scanned on a 7T whole body scanner (Philips Healthcare). Z-spectra were acquired in whole brain using a 3D multi-shot gradient-echo (TR/TE/FA = 65ms/7.2ms/12º, EPI factor 7; 40 slices, 3x3x3 mm^3). The saturation pulse was a 1μT, 25ms single-lobe sinc-gauss pulse (208º) in each TR. Z-spectra: 64 offsets frequencies from -20 ppm to 20 ppm with a dense sampling of 0.1 ppm from -5 to 5 ppm. Three regions of the z-spectra (|f| < 1 ppm, f > 10 ppm and f < -10 ppm) were simultaneously fit to a Lorentzian function to fit out direct water saturation[6]. A Lorentzian difference analysis (LDA) was calculated as the difference between the fitted water Lorentzian and the data. Because we do not use asymmetry analysis we use the terminology clean-APT to indicate measured APT without interference from NOE and direct saturation and strongly reduced contributions from MTC asymmetry. T1 pre Gad, post Gad and a T2-FLAIR were acquired the previous day on a 3T clinical scanner.

Results: Fig. 1a shows a corrected z-spectrum with Lorentzian water fit. The LDA is shown in the lower plot for both the tumor and for a region in the contralateral side. The clean-APT range was assigned from 3.3-3.7 ppm and NOE from -3.3 to -3.7 ppm (highest LDA signal). There was a decrease in both the downfield and upfield side of the spectrum (within the light blue rectangles) of the tumor compared to the contralateral side. Fig. 2 shows images for each of the contrasts. The tumor region had a hypointensity in both clean-APT and NOE-CEST and a hyperintensity in the MTR_{asym}. The T1 post Gad was not enhancing and there was a hyperintensity in the FLAIR region within the tumor region.

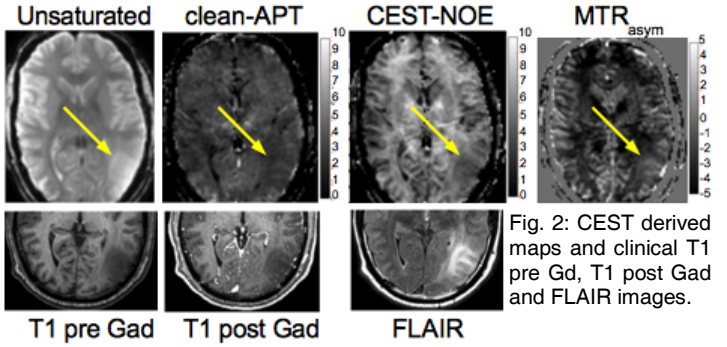

Fig. 2: CEST derived maps and clinical T1 pre Gd, T1 post Gad and FLAIR images.

Discussion: The clean-APT and CEST-NOE images were created without the need for asymmetry analysis and therefore better represent exchangeable mechanisms without cross contamination from other MT effects. The tumor was non-enhancing on T1 post Gad images with FLAIR hyperintensity. Despite intermediate grade, the presence of a reduction in restricted diffusion on the clinical DTI suggests low cellular density. Note that the decrease in both the clean-APT and NOE-CEST images reflects a decrease in the protein content in the voxel, but need not per se reflect a decrease in cellular protein as it is known that cell density in tumors is lower than normal brain tissue due to larger extravascular extracellular space. Previously[1-3], APT quantified from higher power saturation pulses and using the asymmetry analysis showed an increase in the APT-weighted signal compared to normal brain, similar to what was found here in the MTR_{asym}. Originally, MTR_{asym} was defined as APT-weighted[1] having contributions from APT and other MT processes. The increase in APTw images may be due to proportionally decreases in the clean-APT and NOE-CEST signals or from an increase in protein content in the cancer cells that is hard to detect visually in the Z-spectra due to a decrease in overall cell density.

Conclusions: The CEST data were acquired using a low power saturation pulse which makes both the downfield slowly exchangeable protons and the upfield exchange relayed mechanisms visible with no cross-contamination and minimal influence from semisolid macromolecule signal. The signal within the tumor was decreased in both the clean-APT and NOE-CEST images. The MTR_{asym} (APTw) signal was higher as shown previously[1,3].

Refs: 1) Zhou et al. Magn Reson Med 50(6):1120, 2003; 2) Zhou et al., Magn Reson Med 60 (4):842, 2006; 3) Jones et al., Magn Reson Med 56 (3):585, 2006; 4) Zhou et al., Nat Med. 17(1):130, 2011; 5) Desmond & Stanisz MRM 67:979, 2012; 6) Jones et.al., MRM 67:1579, 2012; 7) Ling et.al. PNAS 105:2266, 2008. Funding: NIH grants R01EB015031, R01EB015032, R01EB009731, 1S10 RR028955, P50CA103175 and P41 EB015909